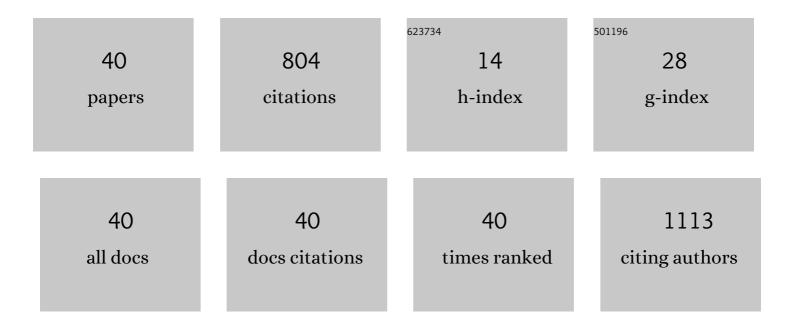
## Xing-Zhao Liu

List of Publications by Year in descending order

Source: https://exaly.com/author-pdf/8203012/publications.pdf Version: 2024-02-01



#	Article	IF	CITATIONS
1	Ultrahigh-Responsivity, Rapid-Recovery, Solar-Blind Photodetector Based on Highly Nonstoichiometric Amorphous Gallium Oxide. ACS Photonics, 2017, 4, 2203-2211.	6.6	254
2	AlN-based piezoelectric micromachined ultrasonic transducer for photoacoustic imaging. Applied Physics Letters, 2013, 103, .	3.3	59
3	High-Temperature SAW Wireless Strain Sensor with Langasite. Sensors, 2015, 15, 28531-28542.	3.8	51
4	Synthesis of few-layer 2H-MoSe <sub>2</sub> thin films with wafer-level homogeneity for high-performance photodetector. Nanophotonics, 2018, 7, 1959-1969.	6.0	41
5	Layer-controlled synthesis of wafer-scale MoSe2 nanosheets for photodetector arrays. Journal of Materials Science, 2018, 53, 8436-8444.	3.7	38
6	PMN-PT/PVDF Nanocomposite for High Output Nanogenerator Applications. Nanomaterials, 2016, 6, 67.	4.1	34
7	The Characterization of Surface Acoustic Wave Devices Based on AlN-Metal Structures. Sensors, 2016, 16, 526.	3.8	34
8	AlN-based surface acoustic wave resonators for temperature sensing applications. Materials Express, 2015, 5, 367-370.	0.5	29
9	AlN-based surface acoustic wave resonators on platinum bottom electrodes for high-temperature sensing applications. Rare Metals, 2016, 35, 408-411.	7.1	26
10	Characterization of Molybdenum Oxide Thin Films Grown by Atomic Layer Deposition. Journal of Electronic Materials, 2018, 47, 6709-6715.	2.2	25
11	High performance photodetectors constructed on atomically thin few-layer MoSe2 synthesized using atomic layer deposition and a chemical vapor deposition chamber. Journal of Alloys and Compounds, 2019, 785, 951-957.	5.5	21
12	Effects of AlN Coating Layer on High Temperature Characteristics of Langasite SAW Sensors. Sensors, 2016, 16, 1436.	3.8	20
13	Growth characteristics and device properties of MOD derived β-Ga2O3 films. Journal of Materials Science: Materials in Electronics, 2014, 25, 3629-3632.	2.2	18
14	Improvement of High-Temperature Stability of Al2O3/Pt/ZnO/Al2O3 Film Electrode for SAW Devices by Using Al2O3 Barrier Layer. Materials, 2017, 10, 1377.	2.9	17
15	The optical properties of alumina films prepared by electron beam evaporation at oblique incidence. Materials Letters, 2013, 101, 1-4.	2.6	14
16	Novel AlN/Pt/ZnO Electrode for High Temperature SAW Sensors. Materials, 2017, 10, 69.	2.9	14
17	AIN film SAW resonator integrated with metal structure. Electronics Letters, 2015, 51, 379-380.	1.0	11
18	Characterization and performance of graphene–PbSe thin film heterojunction. Rare Metals, 2021, 40, 219-224.	7.1	11

2

Xing-Zhao Liu

#	Article	IF	CITATIONS
19	High temperature characteristics of AlN film SAW sensor integrated with TC4 alloy substrate. Sensors and Actuators A: Physical, 2016, 249, 57-61.	4.1	10
20	Photoelectric properties of β-Ga2O3 thin films annealed at different conditions. Rare Metals, 2022, 41, 1375-1379.	7.1	9
21	Determination of the Band Alignment of aâ€lGZO/aâ€lGMO Heterojunction for Highâ€Electron Mobility Transistor Application. Physica Status Solidi - Rapid Research Letters, 2017, 11, 1700251.	2.4	7
22	Surfactant-Assisted Hydrothermal Synthesis of PMN-PT Nanorods. Nanoscale Research Letters, 2016, 11, 49.	5.7	6
23	Amorphous InGaMgO Ultraviolet Photo-TFT with Ultrahigh Photosensitivity and Extremely Large Responsivity. Materials, 2017, 10, 168.	2.9	6
24	Dilute-selenium alloying: A possible perspective for achieving p-type conductivity of β-gallium oxide. Journal of Alloys and Compounds, 2022, 891, 161969.	5.5	6
25	Polymer assisted thick single-layer YBa2Cu3O7-δ films prepared with modified TFA-MOD method. Rare Metals, 2014, 33, 594-597.	7.1	5
26	The electrical and morphological properties of magnesium oxide/alumina bilayered thin films prepared by electron beam evaporation at oblique incidence. Applied Surface Science, 2014, 292, 665-669.	6.1	5
27	Comparative study on the doping effect of 3d elements in Bi1.5Pb0.2Sr2Ca2Cu2.8M0.2O y (M=Sc, Ti, V,) Tj E1	Qq1_1_0.78	343]4 rgBT (O
28	Tailoring the Band Alignment of Ga <sub>x</sub> Zn <sub>1-x</sub> O/InGaZnO Heterojunction for Modulation-Doped Transistor Applications. Physica Status Solidi (A) Applications and Materials Science, 2018, 215, 1800332.	1.8	4
29	Dielectric thin films for GaN-based high-electron-mobility transistors. Rare Metals, 2015, 34, 371-380.	7.1	3
30	Nano-structured optical hetero-coatings for ultraviolet protection. Materials Letters, 2015, 152, 290-292.	2.6	3
31	Effects of the magnesium oxide thin films' microstructures on the residual stresses. Journal of Alloys and Compounds, 2016, 679, 122-124.	5.5	3
32	Two-dimensional MoSe2/graphene heterostructure thin film with wafer-scale continuity via van der Waals epitaxy. Chemical Physics Letters, 2020, 755, 137762.	2.6	3
33	Fabrication of Topological Insulator Bi 2 Se 3 â^'PbSe Heterojunction Photodetector for Infrared Detection. Physica Status Solidi - Rapid Research Letters, 2021, 15, 2100406.	2.4	3
34	van der Waals growth of PbSe thin films on graphene and Bi2Se3. Vacuum, 2022, 201, 111043.	3.5	3
35	Band alignment and interfacial chemical structure of the HfLaO/InGaZnO4 heterojunction investigated by x-ray photoelectron spectroscopy. Journal Physics D: Applied Physics, 2017, 50, 145106.	2.8	2
36	Investigation on band alignment of Bi2Se3–PbSe heterojunction. Applied Physics Letters, 2021, 118, 162101.	3.3	2

#	Article	IF	CITATIONS
37	RESIDUAL STRESSES IN OBLIQUE INCIDENCE DEPOSITED ALUMINA THIN FILM. Surface Review and Letters, 2014, 21, 1450024.	1.1	1
38	Electrical performance of alumina films made in EB evaporation. Modern Physics Letters B, 2016, 30, 1650260.	1.9	1
39	Pyrochlore oxide Y2Hf2O7 thin films for solar-blind UV detectors. Optical Materials, 2020, 105, 109837.	3.6	1
40	Highly orientated Bi(Pb)SrCaCuO superconducting thin film by magnetron sputtering of three targets. Journal of Materials Science Letters, 1996, 15, 531-533.	0.5	0